Stereo Imaging of VHE Gamma-Ray Sources

F.A. Aharonian and A.K. Konopelko[1]

Max-Planck-Institut für Kernphysik, Heidelberg, Germany

Abstract

We describe the features of the stereoscopic approach in the imaging atmospheric Cherenkov technique, and discuss the performance of future low threshold telescope arrays.

1. Introduction

The high detection rate, the ability of effective separation of electromagnetic and hadronic showers, and good accuracy of reconstruction of air shower parameters are three remarkable features of the imaging atmospheric Cherenkov telescope (IACT) technique (see e.g. Cawley and Weekes 1996, Aharonian and Akerlof 1997). The recent reports about detection of TeV γ-rays from several objects by nine groups running imaging telescopes both in the northern (Whipple, HEGRA, CAT, Telescope Array, CrAO, SHALON, TACTIC) and southern (CANGAROO, Durham) hemispheres confirm the early expectations concerning the potential of the technique (Weekes and Turver 1977, Stepanian 1983, Hillas 1985), and provide a solid basis for the ground-based gamma ray astronomy (Weekes et al. 1997a).

In particular, the Whipple 10 m diameter imaging telescope, today's most sensitive single telescope, provides detection of more than 100 γ-rays from the Crab with $\simeq 7$ standard deviation statistical significance within only 1 h observation of the source. Thus the 100 h source exposure by this instrument should be enough to reveal point γ-ray sources above 250 GeV at the flux level of 0.07 Crab. On the other hand, the '7-sigma-per-1 hour' signal from the Crab implies that any short outburst of a TeV source at the level exceeding the Crab flux can be discovered during the observation time of less than 30 minutes. This important feature of the IACT technique was convincingly demonstrated by the Whipple group when two dramatic flares from Mrk 421 were detected in May 1996 (Gaidos et al. 1996). Significant improvement of the performance of this telescope is expected in 1998, after installation a new, 541-pixel high resolution camera (Lamb et al. 1995a).

While the cameras with relatively modest pixel size of about 0.25° provide an adequate quality of imaging of air showers produced by TeV γ-rays (Plyasheshnikov and Konopelko 1990, Zyskin et al. 1994, Aharonian et al. 1995), a smaller pixel size is preferable *(a)* for lowering the energy threshold, and *(b)* for extending the dynamical range towards the higher energies by observations of γ-ray sources at *large zenith angles*. Both possibilities recently have been demonstrated respectively by CAT (Goret et al. 1997) and CANGAROO (Tanimori et al. 1997) groups.

Further qualitative improvement of the IACT technique in the next few years is likely to proceed in two (complementary) directions: (a) implementation of the so called *stereo imaging*, and (b) reduction of the energy threshold towards the sub-100 GeV domain.

[1]Permanent address: Altai State University, Barnaul, Russia

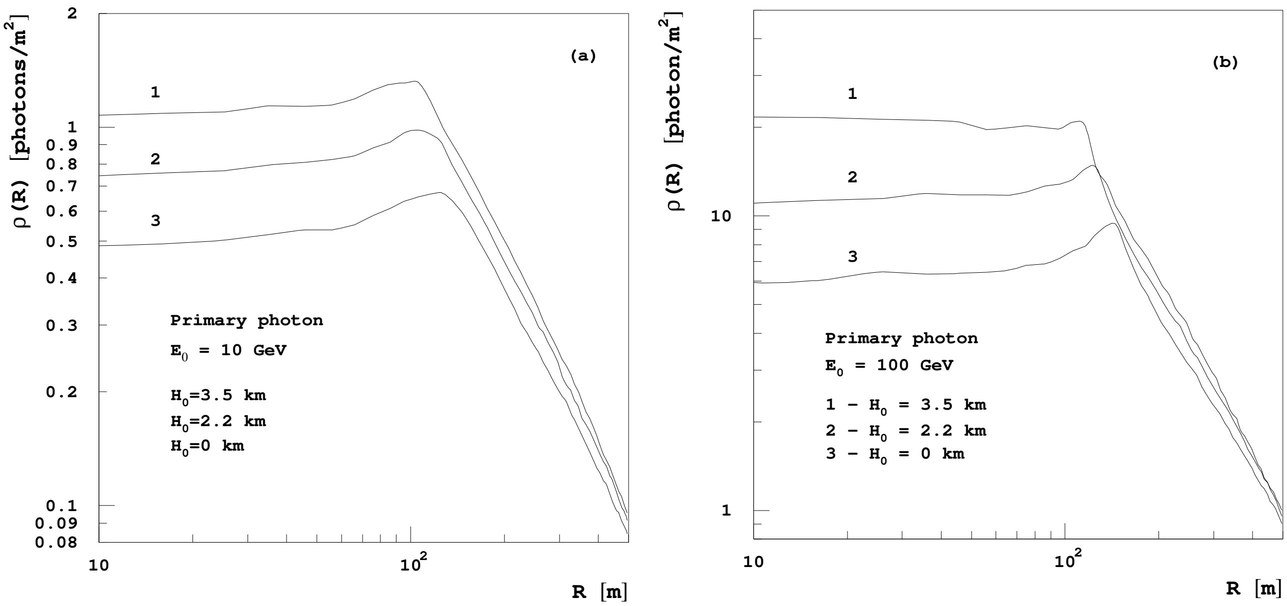

Fig. 1: Density of Cherenkov light photons in 10 GeV and 100 GeV γ-ray showers as a function of the radial distance from the shower core.

2. Stereoscopic Approach

The concept of stereo imaging is based on the simultaneous detection of air showers in different projections by at least two telescopes separated at a distance comparable with the radius of the Cherenkov light pool, $R_{\rm C} \sim 100\,{\rm m}$ (see Fig. 1). Compared to single telescopes, the stereoscopic approach allows (*i*) unambiguous and precise reconstruction of the shower parameters on an *event-by-event* basis, (*ii*) superior rejection of hadronic showers, and (*iii*) effective suppression of the background light of different origins – night sky background (*N.S.B.*), local muons, *etc* (Aharonian et al. 1993, Aharonian 1993, Krennrich and Lamb 1995, Stepanian 1995, Chadwick et al. 1996, Aharonian et al. 1997).

The (only) *disadvantage* of the stereoscopic approach is a significant loss of the detection rate due to the overlap of the shower collection areas of individual telescopes located from each other at distances $\leq 2R_{\rm C}$. However, the loss in statistics is partially compensated, especially for steep spectra of primary γ-rays, by reduction of the energy threshold of the telescopes operating in the coincidence mode.

While the effective collection area of a single telescope is determined by the radius of the Cherenkov light pool, the shower integration area of a multi-telescope system is due to the total geometrical area of the array which may be gathered from individually triggered groups of telescopes – IACT *cells* (Aharonian et al. 1997). The compromise between two principal conditions, namely (a) detection of γ-ray induced showers by several telescopes of the *cell* and (b) minimization of correlation between images in different telescopes, dictate the linear size of the *cell*: $L \simeq R_{\rm C}$. The design of the IACT *cell* depends on the specific detection requirements. However, since the accuracy of reconstructed shower parameters continues to be improved noticeably up to 3 or 4 telescopes in coincidence (Aharonian et al. 1997), the optimum design of the *cell* seems to be a triangular or quadrangular arrangement of IACTs. The concept of the IACT *cell* makes straightforward and rather general the predictions concerning the performance of multitelescope arrays.

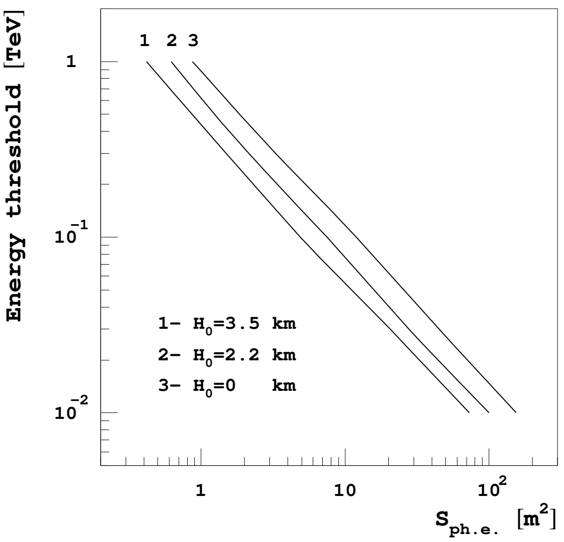

Fig. 2: Energy threshold of an imaging Cherenkov telescope versus the telescope's aperture $S_{\rm ph.e.}$.

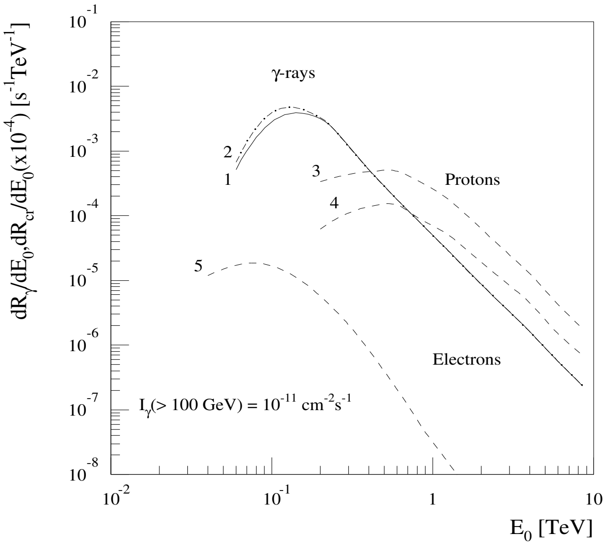

Fig. 3: Differential detection rates of γ*-rays from a point source with differential power-law index 2.5 and integral flux* $J_\gamma(\geq 100\,{\rm GeV}) = 10^{-11}\,{\rm ph/cm^2 s}$*, as well as detection rates of isotropic cosmic ray protons and electrons (*$\times 10^{-4}$*) for the 4-fold telescope coincidence. The curves 2 and 4 are calculated for a camera with pixel size of* $0.15°$*. All other curves are calculated for the pixel size* $0.25°$.

The *effective energy threshold* of the imaging telescopes, $E_{\rm th}$, is basicly determined by two conditions: (*i*) the accidental trigger rate due to the *N.S.B.* should not exceed the detection rate of γ-rays, and (*ii*) the number of photoelectrons in image should be sufficient for proper image analysis; typically $n_{\rm ph.e.}^{\rm (min)} \sim 100$.

Effective suppression of the *N.S.B.* in the IACT technique is provided by the trigger criterion which requires signals above threshold in several adjacent pixels. Since the minimum number of pixels in coincidence is limited by the characteristic image size, the high resolution cameras with pixel size of about $0.1°$ have a certain advantage from the point of view of lowering the energy threshold by using higher trigger multiplicity.

Meanwhile, the disadvantage of (more economical) cameras with relatively large (e.g. $0.25°$) pixel size can be effectively compensated by the requirement of simultaneous detection of a shower by ≥ 2 telescopes with a local 2-pixel coincidence trigger condition. Due to the flat lateral distribution of the Cherenkov radiation of γ-ray showers this requirement does not affect the γ-ray detection efficiency if the distance between telescopes does not exceed 100 m. Assuming now that the *local* and the *system* triggers eliminate effectively the *non-air-shower* backgrounds, the threshold $E_{\rm th}$ could be estimated from the condition (*ii*), namely from the equation $n_{\rm ph.e.}^{\rm (min)} = \rho(E) \times S_{\rm ph.e.}$, where $\rho(E)$ is the density of the Cherenkov photons at plateau produced by a primary γ-ray of energy E, and $S_{\rm ph.e.}$ is the telescope aperture for the number of detected photoelectrons, $S_{\rm ph.e.} = S_{\rm mir} \cdot \chi_{\rm ph \to e}$. Here $S_{\rm mir}$ is the geometrical area of the optical reflector and $\chi_{\rm ph \to e}$ is the so-called 'photon-to-photoelectron' conversion factor, determined by quantum efficiency of the light detectors, the reflectivity of the mirror, *etc.* If for order-of-magnitude estimates one assumes that $\rho(E) \simeq \rho_0 E$, the condition $n_{\rm ph.e.}^{(\rm min)} = 100$ gives, for example at 2 km above see level, $E_{\rm th} = 100\,(S_{\rm ph.e.}/10\,{\rm m}^2)^{-1}$ GeV. In Fig. 2 we show accurate calculations of the dependence of $E_{\rm th}$ on the telescope aperture $S_{\rm ph.e.}$ for different altitudes.

From Fig. 2 one may conclude that the energy threshold around 100 GeV can be achieved, in principle, by a system of 10 m diameter IACTs equipped with conventional PMT based cameras with typical $\chi_{\rm ph\to e} = 0.15$. The Monte Carlo calculations of detection rates for quadrangular 100 m $\times$ 100 m *cell* consisting of four IACTs with aperture $S_{\rm ph.e.} = 10\,{\rm m}^2$ show that the detection rate of γ-ray showers, with the cores inside the *cell*, indeed peaks at 100 GeV (Fig. 3). The efficiency of detection of 100 GeV photons even in the stringent 4-fold telescope coincidence mode is about 50%, and reaches the 100% level already at 200 GeV.

Note that $n_{\rm ph.e.}^{(\rm min)} = 100$ is a rather conservative condition. For relatively strong γ-ray sources, when a comprehensive image analysis is not required, the energy threshold can be lowered down to 50 GeV.

2.2. Reconstruction of Shower Parameters

The procedure of reconstruction of the arrival direction and core position of γ-ray showers by 4 telescopes of the *cell* is demonstrated in Fig. 4. Although one pair of detected images is sufficient to determine unambiguously the shower parameters (except for the events close to the line connecting two telescopes), the information from other images significantly improves the accuracy of estimated shower parameters.

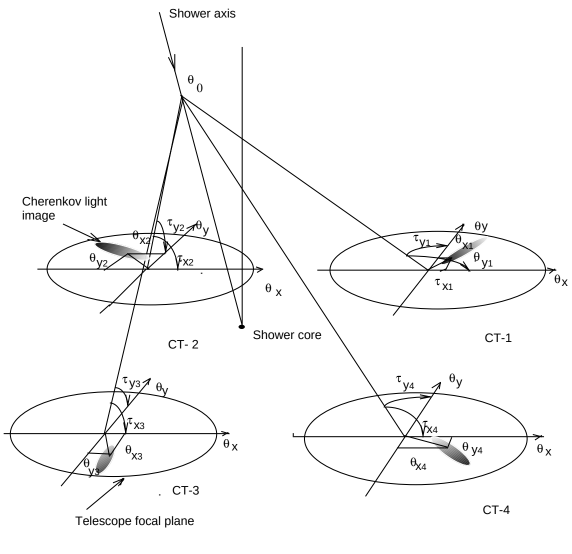

Fig. 4: Reconstruction of the shower parameters by the 4-IACT cell.

The one dimensional angular distributions of showers produced by γ-rays from a point source with energy $E = 100$ GeV, 300 GeV, and 1 TeV are shown in Fig. 5a. The two-dimensional distribution of the reconstructed directions of γ-rays from a point source with E^{-2} spectrum is shown in Fig. 6. The values of the '1σ' angular resolution (68% acceptance of γ-ray showers), are presented in Table 1.

Detection of the shower images by ≥ 2 telescopes allows precise determination of the shower core position (impact parameter). The distributions of uncertainties in reconstructed impact parameter for different primary energies are shown in Fig. 5b. The half width at half maximum (HWHM) values derived from these distributions are presented in Table 1.

Determination of the shower core position with accuracy ≤ 10 m is quite sufficient, due to the flat lateral distribution of the Cherenkov light from the γ-ray showers (see Fig. 1), for the accurate evaluation of the energy using a relation between the primary energy E and the total number of photoelectrons in the image. The accuracy of the energy estimate is essentially due to the fluctuations which are large ($\geq 30\%$) for very close ($R \leq 60$ m) as well as distant ($R \geq 120$ m) showers (see Konopelko 1997). However, most of the showers required to be

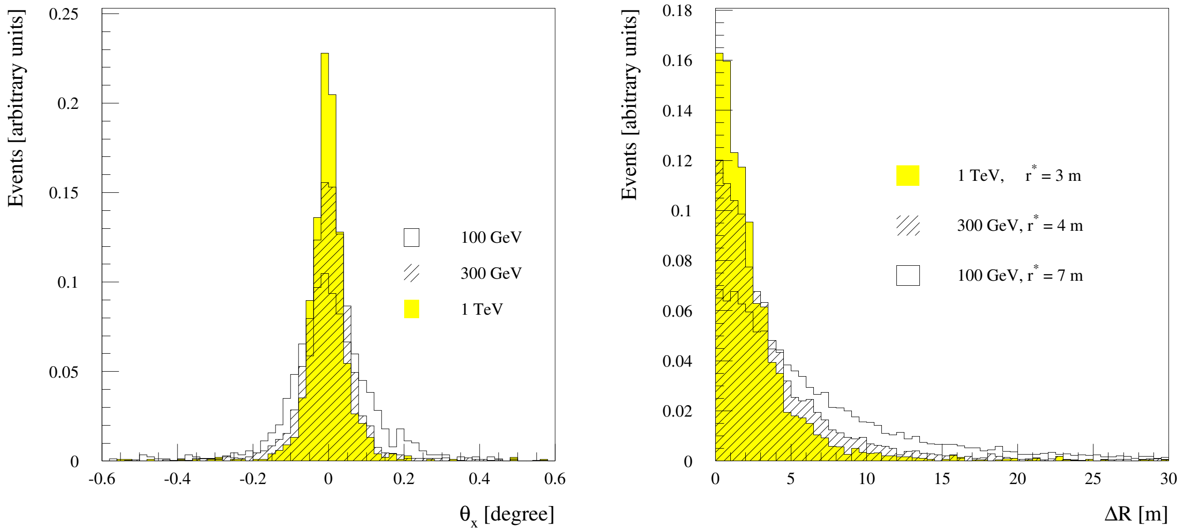

Fig. 5: a (left): One-dimensional angular distribution of γ-ray showers. b (right): Uncertainties in the reconstructed impact parameter of γ-ray showers.

detected by all four telescopes are located between 60 m and 120 m from at least 2 telescopes of the *cell*. Therefore the fluctuations appear to be small enough to provide determination of the energy of γ-ray showers with an accuracy of about 20% in the broad energy range from 100 GeV to 1 TeV (see Table 1).

2.3. Gamma/Hadron Separation

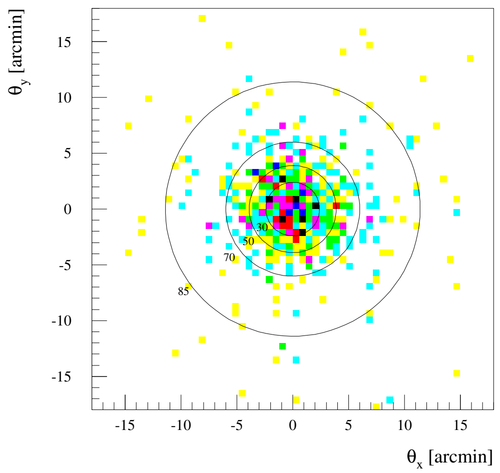

Fig. 6: Two dimensional distribution of reconstructed arrival directions of γ-rays from a point source with the differential spectrum $dJ_\gamma/dE \propto E^{-2}$. Circles correspond to the 30%, 50%, 70%, 85% *γ-rays acceptance.*

Determination of the arrival direction of individual γ-ray showers with an accuracy $\leq 0.1°$ allows effective suppression of the cosmic ray background for point sources by a factor of $\kappa_{\rm cr}^{\rm (dir)} = (2\delta\theta/Psi)^2$, where Ψ is the the angular diameter of the 'trigger zone'. For point sources typically $\Psi \sim 3°$, thus $\kappa_{\rm cr}^{\rm (dir)} \simeq 1/300$. Further improvement of the signal-to-noise ratio is provided by exploitation of the intrinsic differences between the development of the electromagnetic and hadronic cascades. These differences, caused by the large transverse momenta of the secondary hadrons, the deeper penetration of the hadronic cascades into the atmosphere, and essential fluctuations in the hadronic cascades (e.g. Hillas 1996), are effectively transferred to to the shape of the Cherenkov light images. The γ-ray images have compact shape and regular structure, in contrast to rather diffuse and chaotic images of the hadronic showers. For *single* telescopes this provides rejection

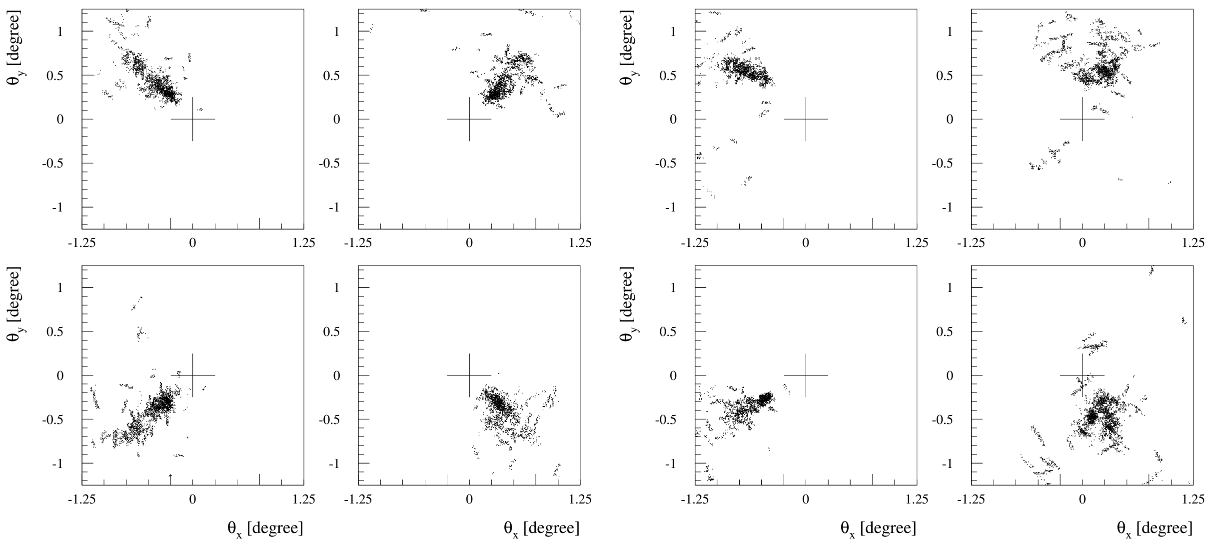

Fig. 7: Cherenkov light images of vertical 100-GeV γ-ray (left) and 300-GeV proton (right) detected by four telescopes of a 100 m $\times$ 100 m IACT cell. Both showers cross the center of the cell. While the images of the proton shower in two telescopes look like γ-ray showers (narrow and regular), the images obtained by two other telescopes clearly indicate the hadronic nature of the shower.

of hadronic showers, based on the so-called *shape* cuts, by a factor of 10 or so (see e.g. Fegan 1997).

Determination of the arrival direction, energy and core location of showers on an *event-by-event* basis with accuracy $\leq 20\%$, $\leq 0.1°$, and $\leq 10\,$m, respectively, allows an optimization of the image 'cuts' which separate the CR and γ-ray domains in the shower parameter space, and thus improves the rejection efficiency for hadronic showers. Furthermore, even though the images in different projections are not entirely independent of each other, the correlation is only partial. Therefore, the joint analysis dramatically improves the gamma/hadron separation power (this effect is demonstrated in Fig. 7). The characteristic values of the acceptance of γ-ray (κ_γ) and proton ($\kappa_{\rm h}$) induced showers, as well as the so-called Q-factor, $Q = \kappa_\gamma/\kappa_{\rm h}^{1/2}$ (the enhancement of the signal-to-noise ratio after the application of the cuts; see, e.g. Fegan 1997), are presented in Table 2.

Table 1: The angular, distance, and energy resolutions of the 4-IACT cell.

	100 GeV	300 GeV	1 TeV
σ_θ, arcmin	6	4.5	3
δr, m	3	4	7
$\delta E/E$, %	20	20	22

It is seen that rejection efficiency of hadronic showers significantly increases with the number of detected images, and under the condition of 50% acceptance of γ-ray events the rejection factor $\kappa_{\rm h}^{-1}$ of 4-IACT *cell* can be as large as 300. This results in the Q-factor of about

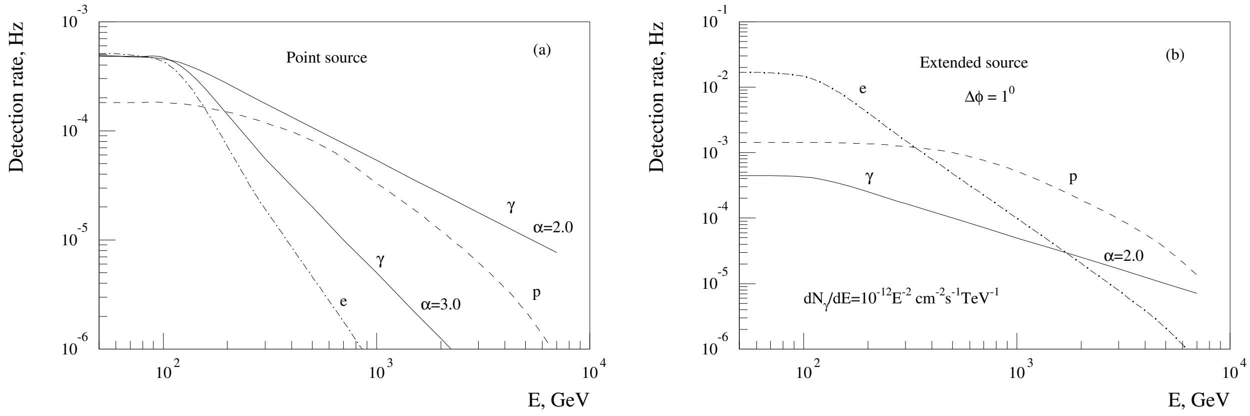

Fig. 8: Detection rates of γ-rays (solid lines), as well as cosmic ray protons (dashed) and electrons (dot-dashed) by the 100 *m* $\times$ 100 *m IACT cell, after application of software image cuts. (a) – point source, and (b) – '*1°*' diffuse source of γ-rays. In both cases an integral flux of γ-rays* $J_\gamma(\geq 100\,\mathrm{GeV}) = 10^{-11}\,\mathrm{ph/cm^2s}$ *with power-law indices $\alpha = 2$ and $\alpha = 3$ is assumed. In the case of point sources the combined* 50% *acceptance for γ-rays is achieved by applying directional and relaxed shape cuts, while in the case of a '*1°*' source the same* 50% *γ-ray acceptance is a result of tight shape cut.*

8. Note that such effective gamma/hadron separation is provided by application of a 'scaled' *Width* parameter (Konopelko 1995). The other parameters, like image *Length*, time structure, UV-content of the Cherenkov light flashes, *etc.*, are less effective, but they still can improve the efficiency of suppression of the hadronic showers being applied separately. However, in the case of stereoscopic observations, the *Width* cuts in different projections are so effective, that they practically do not leave a room for further enhancement of the signal (Aharonian et al. 1997).

The suppression of the cosmic ray background based on the *directional* and *shape* criteria for point sources could be as effective as $\kappa_{\rm cr} = \kappa_{\rm cr}^{\rm (dir)} \kappa_{\rm h} \simeq 10^{-5}$ with the Q-factor close to 100. For comparison, CR rejection efficiency and Q-factor in case of single IACTs, after the application of both *orientational* (*Alpha*) and *shape* cuts, hardly can exceed 10^{-3} and 10, respectively.

Due to the high rejection efficiency of hadronic showers by the IACT *cell*, the cosmic ray

Table 2: CR background rejection efficiency of IACT 'cell' using parameter Width with and without 'scaling'. In the analysis the N-fold Width cuts were used (N = 2,3,4; N is the number of the images passed the cut).

Parameter:	Scaling:		2	3	4
		κ_γ	0.792	0.585	0.489
Width	No	$\kappa_{\rm h}$	0.116	0.038	0.016
		Q-factor	2.32	3.00	3.87
		κ_γ	0.891	0.634	0.490
Width	Yes	$\kappa_{\rm h}$	0.076	0.017	0.0036
		Q-factor	3.23	4.86	8.33

background at energies below 200 GeV is dominated by showers produced by electrons (see Fig.8 a,b). This allows detection of γ-rays from point sources under almost *background-free* conditions if the photon flux above 100 GeV exceeds 10^{-11} ph/cm^{2}s (approximately 1/20 of the Crab flux expected at these energies).

3. HEGRA: The Stereo Imaging Does Work !

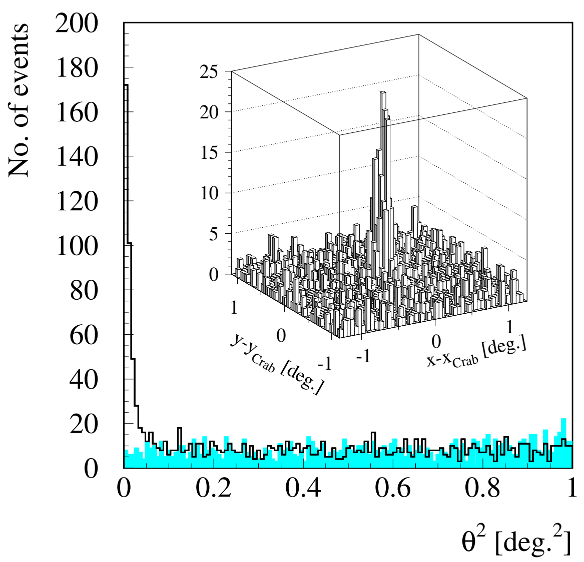

Fig. 9: Distribution of the reconstructed directions of the showers detected from the Crab by the HEGRA IACT system (from Daum et al. 1997).

The recent observations of the Crab Nebula and Mrk 501 by HEGRA stereoscopic system of 4 IACTs (Daum 1997, Herman 1997, Hofmann 1997) confirm the early predictions for the performance of the instrument (Aharonian 1993). Fig. 9 shows the angular distribution of showers detected from the direction of the Crab, and selected after the image *shape* cuts (Daum et al. 1997). The confinement of the γ-ray signal from a point source in a very small angular region (with radius $\sim 0.1^\circ$) of the available two-dimensional phase space, in addition to the significant suppression of hadronic showers at the *trigger* level, results in a strong 4σ-per-1 h signal already before the gamma/hadron separation. The *shape* cuts provide further, by a factor of 100, suppression of the hadronic background, while maintaining the efficiency of the acceptance of γ-ray events at the level of 50%. This leads to only $\simeq 1$ background event in the 'signal' region while the rate of γ-rays from the Crab exceeds 20 events/h. This enables (*i*) an effective search for VHE γ-ray point sources with fluxes down to 0.1 Crab at almost *background free* conditions, and thus allows drastic reduction of the observation time (by a factor of 10) compared to four independently operating telescopes, (*ii*) detailed spectroscopy of strong (Crab-like) VHE emitters, (*iii*) study of the spatial distribution of γ-ray production regions on arcminute scales, (*iv*) effective search for *extended* sources with angular size up to $\simeq 1^\circ$ at the flux level of 0.1 Crab. The exploitation of the 'nominal' 5-IACT HEGRA system with improved trigger condition should allow 5σ detection of faint γ-ray sources at the flux level of 0.025 Crab (Aharonian 1997, Hofmann 1997) which corresponds to $\simeq 10^{-12}$ erg/cm^{2}s energy flux above the effective energy threshold of the instrument of about 500 GeV.

4. Future 100 GeV Class IACT Arrays

One of the principal issues for future detectors is the choice of the energy domain. If one limits the energy region to a relatively modest threshold around 100 GeV, the performance of IACT arrays and their practical implementation can be prediced with high confidence. In practice, an energy threshold of 100 GeV can be achieved by a stereoscopic system of IACTs consisting of 10 m diameter optical reflectors equipped with conventional PMT-based high resolution cameras. Two such arrays of 10 m class telescopes – VERITAS (Weekes et al. 1997b) and HESS (Hofmann 1997) – are likely to be constructed in the foreseeable future.

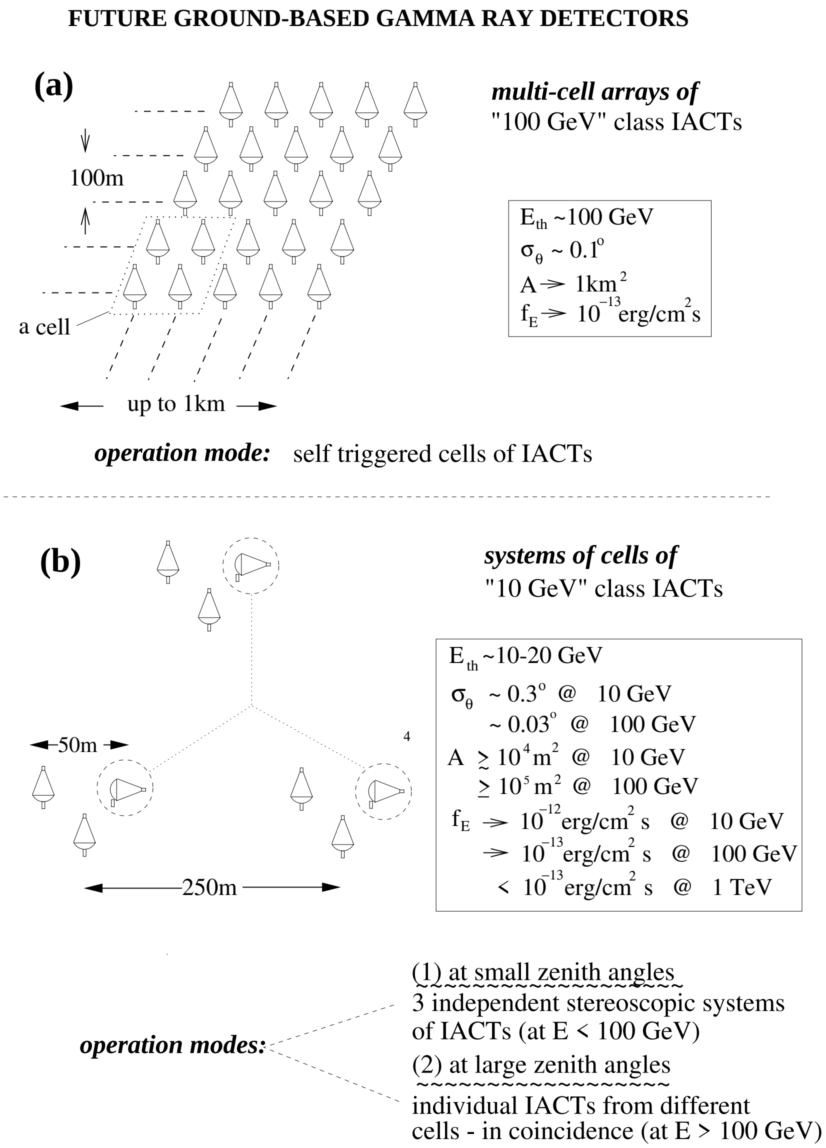

Fig. 10: Two possible arrangements of (a) 100 GeV class and (b) 10 GeV class IACT arrays.

After reaching the maximum possible suppression of the cosmic ray background by simultaneous detection of the air showers in different projections – limited basically by intrinsic fluctuations in cascade development – the further improvement of the flux sensitivities for a given energy threshold can be achieved by increasing the shower collection area, i.e. the number of IACT *cells*. A possible arrangement of a cell-structured array is schematically shown in Fig. 10a. For the arrays consisting of a large number of *cells*, e.g. $n_0 > 10$, and for a given observation time t_0, the minimum detectable flux of γ-rays from a source of angular size ϕ is determined essentially by the product $A = n_0 \times t_0$ from the following two conditions: (1) high confidence level of a γ-ray signal, i.e. $\sigma = R_\gamma (R_\mathrm{p} + R_\mathrm{e})^{-1/2} A^{1/2} G^{-1}(\phi) \geq \sigma_0$, and (2) adequate

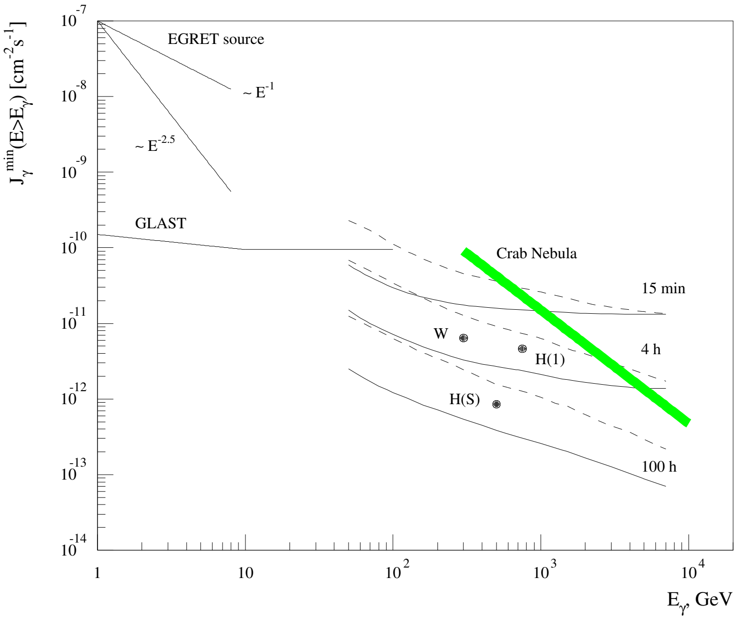

Fig. 11: Minimum detectable fluxes of γ-rays from a point source (solid lines) and $1°$ source (dashed lines) within 100 h observation time by an array consisting of twenty five 10 m diameter IACT cells. The calculations correspond to the requirement of a 5σ γ-ray signal with at least 25 detected photons. For comparison, we show the following fluxes: (i) power-law extrapolations of a 'standard' EGRET source with integral indices $(\alpha - 1) = 1$ and 2.5; (i) the level of the measured γ-ray fluxes of the Crab Nebula above 300 GeV, assumed in the form of $\mathrm{J_{Crab}}(\geq \mathrm{E}) \simeq 1.5 \times 10^{-11}\,(\mathrm{E}/1\,\mathrm{TeV})^{-1.5}\,\mathrm{ph/cm^2s}$. *The minimum detectable fluxes of γ-rays by the single HEGRA and Whipple telescopes (indicated as H(1) and W, respectively), and by the HEGRA IACT system (H(S)), calculated for 100 h observations of a point source, are also shown.*

photon statistics, i.e. $N_\gamma = R_\gamma A \geq N_0$. Here R_γ, $R_{\rm p}$, and $R_{\rm e}$ are the detection rates of γ-rays from a point source, and the detection rates of cosmic ray protons and electrons by one IACT *cell*, respectively (see Fig. 8a). The parameter $G(\phi) \simeq \max[1, \phi/\delta\theta]$ takes into account the angular size of the source. In Fig. 11 we show the minimum detectable γ-ray fluxes from a point source and $1°$ source requiring $\geq 5\sigma$ appearance of a signal, provided that the number of detected γ-rays exceeds 25. Note that at a large exposure, e.g. $A \geq 2500\,\mathrm{h}$, which can be realized, for example, by 100 h observations of a source with an array consisting of 25 IACT-*cells*, $J_\gamma^{\rm min}(\geq 100\,\mathrm{GeV}) \sim 10^{-12}\,\mathrm{ph/cm^2s}$, or the corresponding energy flux $f_{\rm E} \sim 10^{-13}\,\mathrm{erg/cm^2s}$.

At a small exposure, e.g. $A = n_0 \times t_0 \leq 100\,\mathrm{h}$, the minimum detectable fluxes are limited, especially at high energies, by low γ-ray statistics. This could be treated as a disadvantage of cell-structured arrays with fixed linear size of the *cell*, since such arrays with $L \sim R_{\rm C} \sim 100\,\mathrm{m}$ are optimized, to a large extent, to the energy region close to the threshold. Indeed, although the homogeneous multi- cell arrays provides rather economical coverage of large detection areas at the threshold energies (each telescope is exploited by four *cells*), at high energies this concept becomes less effective. Namely, it cannot use the advantage that the showers initiated by high energy photons, $E \gg E_{\rm th}$, can be detected at distances well beyond 100 m. However this disadvantage of homogeneous cell-structured arrays can be compensated, at least partially, by observations at large zenith angles by ≥ 2 telescopes in coincidence from different peripheries of the array.

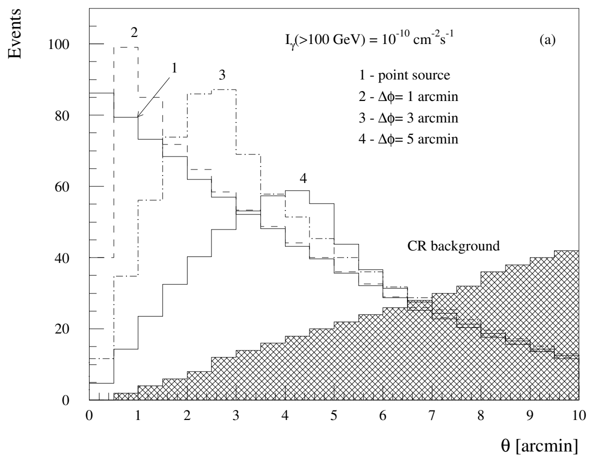

Fig. 12: Distributions of the reconstructed arrival directions of γ-rays from sources with different angular radius. The histogram 1 corresponds to the two-dimensional distribution shown in Fig. 6.

From this point of view it would be important to equip some of the telescopes of the array, located at large distances from each other, by very high resolution cameras with pixel size $\simeq 0.1^\circ$.

The determination of arrival directions of γ-rays by IACT arrays on an *event-by-event* basis with accuracy $\leq 0.1^\circ$ makes possible a study of the spatial distribution of VHE γ-ray sources in arcminute scales. This is demonstrated in Fig. 12, where the distributions of the angular distance of reconstructed directions of γ-rays from the center of extended source are shown. From this figure we may conclude that for sufficiently high photon statistics (say $\geq 10^3$ detected γ-rays) it would be possible to measure the size of an extended source of $\phi \leq 0.1^\circ$ with accuracy ≤ 1 arcmin.

Good energy resolution of about $\delta E/E \sim 20\%$ enables reasonable spectrometry with IACT arrays with ability, for example, to reveal spectral features like sharp cutoffs in the spectra of VHE sources (see Fig. 13).

Due to very effective rejection of the hadronic showers by the stereoscopic IACT systems, the cosmic ray background at energies close to 100 GeV is dominated by the showers produced by primary electrons. This component of electromagnetic showers remains as a part of the background which principally cannot be removed, and thus it is the most serious limiting factor of flux sensitivities, especially for extended sources. On the other hand, these electromagnetic showers with known flux and spectrum of the primary electrons, measured up to energies 1 TeV (Nishimura et al. 1980), can be used for absolute *energy calibration* of the IACT arrays. Although the current uncertainties in 100 GeV electron fluxes could be as large as factor of 2, the future balloon and satellite measurements (e.g. Torii et al. 1997, Müller et al. 1997, Ormes et al. 1997), should be able to reduce significantly the flux uncertainties.

The energy calibration by using the cosmic ray electrons provides unique tool for the *continuous* (on-line) control of the characteristics of IACT arrays (e.g. the energy threshold, the detection area, *etc.*) during the γ-ray observations. For example, 10 min exposure will be enough for detection of more than 100 electrons within the field of view of 100 GeV threshold array consisting of 9 IACT *cells* (see Fig. 8b). It is difficult to overestimate the significance of such calibration and control, especially for the study of the spectral characteristics of highly variable γ-ray sources on sub-hour timescales.

5. Sub-100 GeV Ground-Based Detectors

The strong scientific motivations to fill the gap between the space-based and ground based observations recently stimulated several interesting proposals for extending the atmospheric

Cherenkov technique down to 10 GeV region (see e.g. Lamb et al. 1995b). Among a variety of competing projects this goal could be addressed by the stereoscopic systems of IACTs with the telescope apertures of $S_{\rm ph.e.} \geq 50\,{\rm m}^2$. With development of the technology of novel, fast optical detectors of high quantum efficiency ($\chi_{\rm ph \to e} \geq 50\%$) and design of (relatively inexpensive) 20 m class reflectors with an adequate optical quality for the Cherenkov imaging on scales of several arcminutes, it would be possible to reduce the detection threshold down to 20 GeV, or even 10 GeV for systems installed at high mountain elevations (e.g. 3.5 km a.s.l). Considerable R&D efforts, in particular by the Munich group (Lorenz 1997, Mirzoyan 1997) are already started in both directions. It is expected that this activity will result in construction of a large single reflector telescope (MAGIC) which, together with two ongoing projects of low energy threshold air Cherenkov detectors based on large mirror assemblies of the existing solar power plants – STACEE (Ong et al. 1997) and CELESTE (Parè et al. 1997) – will start to explore the energy region below 100 GeV. Moreover, if successful, the MAGIC telescope could be considered as a prototype for the basic element in future (post 'VERITAS/HESS') arrays of 10 GeV class IACTs.

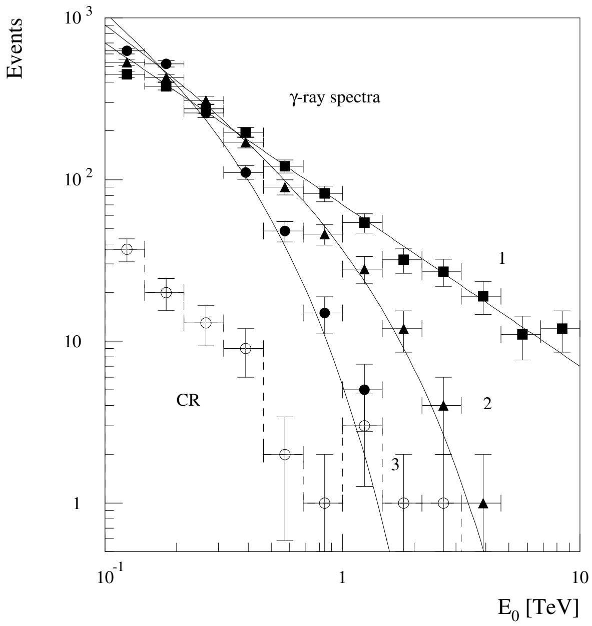

Fig. 13: Evaluation of differential spectra of γ-rays detected by an array for $A = n_0 \times t_0 = 50\,{\rm h}$. The primary spectra (solid lines) have a power-law form $\propto E^{-2.2}$ with different values of a cutoff energy: 1 - $E^\star > 10\,{\rm TeV}$ (corresponding reconstructed fluxes are shown by filled quadrangles); 2 - $E^\star = 1\,{\rm TeV}$ (reconstructed fluxes - filled triangles); 3 - $E^\star = 300\,{\rm GeV}$ (reconstructed fluxes - filled circles). The CR background events, remaining after application of image 'cuts', are shown by open circles.

The efficiency of the imaging technique at energies well below 100 GeV seems to be lower than at higher energies. Indeed, at energies close to 10 GeV, the γ-ray images become less elongated (more circular) and less regular. In practice this means an introduction of significant uncertainties in the reconstruction of the arrival direction of γ-rays, as well as in the gamma/hadron separation strategies. In particular, our preliminary results show that the angular resolution of stereoscopic systems at 10 GeV hardly can be better than 0.2°. Also, due to large fluctuations in low-energy hadronic showers (especially due to the higher probability of production of a leading π^0 meson which takes almost all energy of the primary hadron), an essential fraction of the cosmic rays could "pass" the *shape* cuts, i.e. could be accepted as γ-rays. On the other hand, since the electron/proton ratio of cosmic rays increases at lower energies as $\propto E^{-0.6}$, the weakened rejection efficiency of hadronic showers seems to be still sufficient for operation of the *stereoscopic* sub-100 GeV IACT systems in the regime when the background is dominated by the cosmic ray electrons. This makes straightforward the prediction for the flux sensitivity of such systems. Indeed, since the showers caused by electrons are quite similar to the γ-ray showers, the condition of detection of 5σ signal of γ-rays with differential spectrum $\mathrm{d}J_\gamma/\mathrm{d}E$ at any energy E within the interval $[E-\Delta E, E+\Delta E]$ results in

$$\left(\frac{\mathrm{d}J_\gamma}{\mathrm{d}E}\right)_{\min} = 5\left(\frac{(\mathrm{d}F_\mathrm{e}/\mathrm{d}E\mathrm{d}\Omega)\Delta\Omega}{2\Delta E t_0 S_\mathrm{eff}(E)\kappa_{\mathrm{e.-m.}}\kappa_\theta^2}\right)^{1/2},$$

where $\mathrm{d}F_\mathrm{e}/\mathrm{d}E\mathrm{d}\Omega \simeq 4\cdot10^{-2}E^{-3.2}\,\mathrm{cm}^{-2}\mathrm{s}^{-1}\mathrm{sr}^{-1}\mathrm{GeV}^{-1}$ is the measured spectrum of the cosmic ray electrons; $S_\mathrm{eff}(E)$ is the effective area of detection of electromagnetic showers, κ_θ and $\kappa_{\mathrm{e.-m.}}$ are the acceptance of electromagnetic showers after application of the *directional* and *shape* cuts; $\Delta\Omega \simeq \pi\sigma_\theta^2$ is the solid angle corresponding to the (1σ) angular resolution of the instrument $\sigma_\theta(E)$ at energy E; and t_0 is the exposure time. For characteristic values $\Delta E = (\delta E/E)E \simeq 0.25E$, $\kappa_{\mathrm{e.-m.}} = 0.5$, $\kappa_\theta = 0.68$, we obtain

$$\left(\frac{\mathrm{d}J_\gamma}{\mathrm{d}E}\right)_{\min} \simeq 1.5\cdot10^{-9}E^{-2.1}\left(\frac{\sigma_\theta(E)}{0.1^\circ}\right)\left(\frac{S_\mathrm{eff}(E)}{10^4\,\mathrm{m}^2}\right)^{-1/2}\left(\frac{t_0}{100\,\mathrm{h}}\right)^{-1/2}\ \mathrm{ph/cm^2\,s\,GeV}.$$

Our preliminary calculations show that with a stereoscopic system consisting of several sub-100 GeV threshold IACTs, we may expect $\sigma_\theta \sim 0.2^\circ$, and $S_\mathrm{eff} \sim 4\times10^4\,\mathrm{m}^2$ at 20 GeV which results in the integral flux sensitivity $J_\gamma(\geq 20\,\mathrm{GeV}) \sim 5\times10^{-11}\,\mathrm{ph/cm^2s}$.

Thus, a few sub-100 GeV imaging telescopes being combined in a stereoscopic system could effectively intervene the domain of satellite-based gamma ray instruments like GLAST (Bloom 1996). But, of course, the scientific goals of these instruments are quite different. If the GLAST with its large (almost 2π) FoV could provide very effective sky surveys, sub-100 GeV ground based instruments have an obvious advantage for the search and study of variable sources. On the other side, sub-100 GeV IACT systems could operate also in the TeV domain by observing the γ-ray sources at large zenith angles. If high efficiency of this technique, that already has been demonstrated by the CANGAROO group at multi-TeV energies, could be extrapolated to the 0.1-1 TeV region, the use of an array consisting of few 10 GeV class IACT systems (with 3 or 4 telescopes in each) could cover very broad energy range extending from 10 GeV to 1 TeV. Note however that more detailed Monte Carlo studies are needed for definite conclusions about the performance of sub-100 GeV stereoscopic IACT systems.

A possible arrangement and operation modes of an array of 10 GeV class telescopes are described in Fig. 10.

6. Summary

The stereoscopic approach in the imaging atmospheric Cherenkov technique provides superior gamma/hadron separation power ($\kappa_\mathrm{h} \leq 10^{-2}$), excellent angular resolution ($\sigma_\theta \leq 0.1^\circ$), good energy resolution ($\delta E/E \sim 20\%$), and impressive flux sensitivity ($\sim 10^{-13}\,\mathrm{erg/cm^2s}$) that makes the multi telescope arrays as very effective tools for the study of the sky in γ-rays in a broad energy region from 10 GeV to $\geq 10\,\mathrm{TeV}$. The recent results obtained by the HEGRA system of imaging telescopes, and by the prototype of the Telescope Array (Teshima 1997) generally confirm the early predictions concerning the performance of the technique in the TeV regime. The forthcoming HESS and VERITAS arrays of 10 m class imaging telescopes, with energy threshold of about 100 GeV or less, will improve the flux sensitivities of current instruments by an order of magnitude, and will enable an effective study of distant extragalactic sources with redshifts up to $z \sim 1$. With development of new technologies of construction of 20 m class optical reflectors and novel high quantum efficiency ($\geq 50\%$) optical detectors, it will be possible to extend the energy domain of the stereoscopic IACT arrays down to 10 GeV. However, it should be emphasized that if the performance of the 100 GeV threshold IACT arrays, and their practical implementation can be predicted with high degree of confidence, the realization of 10 GeV threshold IACT arrays still remains as an exciting challenge.

We thank W. Hofmann, A.V Plyasheshnikov, and H.J. Völk for many fruitful discussions.

References

Aharonian, F.A., Chilingarian, A.A., Mirzoyan, R.G., Konopelko A.K., Plyasheshnikov, A.V. 1993, Experimental Astronomy, 2, 331

Aharonian, F.A. (HEGRA collaboration) 1993, in Proc. "Towards a Major Atmospheric Cherenkov Detector-IV" (Calgary), ed. R.C. Lamb, p.81

Aharonian, F.A., Heusler, A., Hofmann, W., Wiedner, C.A., Konopelko A.K., Plyasheshnikov, A.V., Fomin, V. 1995, J.Phys.. G: Nucl. Part. Phys., 21, 985

Aharonian, F.A. (HEGRA collaboration) 1997, in Proc. 4th Compton Symposium, eds. C.D. Dermer et al., AIP Conf. 410, p.1631

Aharonian, F.A., Hofmann, W., Konopelko, A.K., and Völk, H.J. 1997, Astroparticle Physics, 6, I: p. 343; II: p.369

Aharonian, F.A., and Akerlof, C.A. 1997, Annual Rev. Nucl. Part. Sci., 47, 273

Bloom, E.D. 1996, Space Sci. Rev., 75, 109

Cawley, M.F., and Weekes, T.C. 1996, Experimental Astronomy, 6, 7

Chadwick, P.M. et al. 1996, Space Sci. Rev., 75, 153

Daum, A. 1997, these proceedings

Daum, A. et al. 1997, Astroparticle Physics, in press

Fegan, D.J. 1997, J.Phys.. G: Nucl. Part. Phys., 23, 1013

Gaidos, J.A. et al. 1996, Nature, 383, 319

Goret, P. et al. 1997, in Proc. 25th ICRC (Durban), 3, p.173

Hermann, G. 1997, these proceedings

Hillas, A.M. 1985, in Proc 19th ICRC (La Jolla), 3, p.445

Hillas, A.M. 1996, Space Sci. Rev., 75, 17

Hofmann, W. 1997, these proceedings

Kifune, T. 1997, these proceedings

Konopelko, A.K. 1995, in Proc. "Towards a Major Atmospheric Cherenkov Detector-IV" (Padova), ed. M.Cresti, p.373

Konopelko, A.K. 1997, these proceedings

Krennrich, F., and Lamb, R.C. 1995, Experimental Astronomy, 6, 285

Lamb, R.C. et al. 1995a, in Proc. "Towards a Major Atmospheric Cherenkov Detector-IV" (Padova), ed. M.Cresti, p.386

Lamb, R.C. et al. 1995b, in Proc. "Particle and Nuclear Astrophysics and Cosmology in the Next Millennium", ed. E.W. Kolb and R.D. Peccei (World Scientific, Singapore), p.295

Lorenz, E. 1997, these proceedings

Mirzoyan, R. 1997, these proceedings

Müller, D. et al. 1997, in Proc. 25th ICRC (Durban), 4, p.237

Nishimura, J. et al. 1980, ApJ, 238, 394

Ong, R.A. et al. 1997, these proceedings

Ormes, J.F. et al. 1997, in Proc. 25th ICRC (Durban), 5, p.73

Parè E. et al. 1997, these proceedings

Plyasheshnikov, A.V. and Konopelko, A.K. 1990, in Proc 21st ICRC (Adelaide), 4, p.250

Stepanian, A.A. et al. 1983, Izv. Krym. Astrophyz. Obs., 66, 234

Stepanian, A.A. 1995, Nuclear Physics B, 39A, 207

Tanimori, T. et al. 1997, ApJ, in press

Teshima, M. 1997, private communication

Torii, S. et al. 1997, in Proc. 25th ICRC (Durban), 4, p.241

Weekes, T.C., and Turver, K.E. 1977, in Proc. 12th ESLAB Symposium (Frascati), p.279

Weekes, T.C., Aharonian, F.A., Fegan, D.J., and Kifune, T. 1997a, in Proc. 4th Compton Symposium, eds. C.D. Dermer et al., AIP Conf. 410, p. 361

Weekes T.C. et al. 1997b, in Proc. 25th ICRC (Durban), 5, p.173

Zyskin, Yu. L., Stepanian, A.A., and Kornienko A.P. 1994, J.Phys.. G: Nucl. Part. Phys., 20, 1851